

System reduction-based approximate reanalysis method for statically indeterminate structures with high-rank modification

Wenxiong Li^{*}, Suiyin Chen, Huan Huang^{*}

College of Water Conservancy and Civil Engineering, South China Agricultural University, Guangzhou 510642, China

^{*}Corresponding author. E-mail: leewenxiong@scau.edu.cn (W. Li), happyhuang@scau.edu.cn (H. Huang)

Abstract Efficient structural reanalysis for high-rank modification plays an important role in engineering computations which require repeated evaluations of structural responses, such as structural optimization and probabilistic analysis. To improve the efficiency of engineering computations, a novel approximate static reanalysis method based on system reduction and iterative solution is proposed for statically indeterminate structures with high-rank modification. In this approach, a statically indeterminate structure is divided into the basis system and the additional components. Subsequently, the structural equilibrium equations are rewritten as the equation system with the stiffness matrix of the basis system and the pseudo forces derived from the additional elements. With the introduction of spectral decomposition, a reduced equation system with the element forces of the additional elements as the unknowns is established. Then, the approximate solutions of the modified structure can be obtained by solving the reduced equation system through a pre-conditioned iterative solution algorithm. The computational costs of the proposed method and the other two reanalysis methods are compared and numerical examples including static reanalysis and static nonlinear analysis are presented. The results demonstrate that the proposed method has excellent computational performance for both the structures with homogeneous material and structures composed of functionally graded beams. Meanwhile, the superiority of the proposed method indicates that the combination of system reduction and pre-conditioned iterative solution technology is an effective way to develop high-performance reanalysis methods.

Keywords Structural reanalysis; System reduction; Iterative solution; High-rank modification; Pseudo forces

1. Introduction

Structural reanalysis plays a crucial role in different branches of structural engineering, such as optimization of large-scale structures, structural damage identification, nonlinear structural analysis and probabilistic analysis [1], which require repeated evaluations of structural responses and updating structural parameters. Structural reanalysis methods refer to the analysis method with high computational efficiency for the modified structures by making use of the structural stiffness matrix, the displacement solution of the original structure and other information [2]. In many specific applications, it is necessary to efficiently realize the structural reanalysis under the condition of large range modification or even global modification. Therefore, the development of efficient reanalysis methods for the structures with high-rank modification is a topic of great concern. During the past decades, different structural reanalysis methods have been developed and they are divided into direct methods and approximated methods.

Direct methods aim to directly give the exact solutions to the modified structures. Most of the direct methods are variations on two general matrix-update formulas: the Sherman-Morrison (SM) and Woodbury (SMW) formulas [3]. These formulas could have been used as efficient tools in exact structural reanalysis involving low-rank modifications. Sack et al. [4] used the Sherman-Morrison (SM) formula to compute the inverse of a modified matrix. Krisch and Rubinstein [5] adopted the Woodbury formula to compute the modified inverse and the modified displacement. Akgün [2] presented a review of the development of SMW formulas and investigated the other structural reanalysis methods with the SMW formulas. Huang and Verchery [6] developed another exact method based on the SMW formulas for structural static reanalysis with modifications on structural elements, boundary or loading conditions, independently or in combination. Derived from the Sherman-Morrison-Woodburg formulas, Deng and Ghosn [7] designed the pseudo force solver to enhance the efficiency of structural reanalysis algorithms by avoiding reassembling the global stiffness matrix. In this solver, the response of the modified structure is defined as the difference between the response of the original structure to a set of applied loads and the response of the original structure to a set of pseudo forces. Yang [8] proposed an exact method for structural static

reanalysis following flexibility disassembly perturbation and the SMW formulas, which provides a relatively effective approach for structures with high-rank modification. Besides, some recent researches, such as the exact reanalysis approach of Song et al. [9], the exact block-based reanalysis method of Gao et al. [10], and the enhanced substructure coupling dynamic reanalysis technique of Jensen et al. [11], provide new direct methods for structural reanalysis. Notably, most exact reanalysis methods are only suitable to the structures with low-rank modifications. With regard to the high-rank modification, which is more common in structural optimization design, most direct reanalysis methods are difficult to significantly improve the solution efficiency. In some cases, the computational effort of the reanalysis methods may be even larger than the effort required by a regular complete analysis.

Approximate methods are generally applied to the reanalysis of structures with a large number of changes of small magnitude. From the perspective of implementation mode, approximate methods are divided into two categories: the methods based on the combination of basis vectors and the methods based on the iterative solution process. The combined approximations (CA) method proposed by Kirsch [12] is the most representative method under the concept of a combination of basis vectors. It made considerable contributions to the reanalysis solution procedures for various issues in the last 15-20 years. Kirsch [13, 14] presented a complete, unified and thorough study and review of these reanalysis techniques. There are two complications affecting the applicability of the CA method: how to reasonably determine the number of basis vectors; the solution accuracy for the case of local large modification. The Krylov subspace methods with an iterative process [15], such as Pre-conditioned Conjugate Gradient method (PCG), Generalized Minimum Residual algorithm (GMRES) and Bi-Conjugate Gradient Stabilized algorithm (Bi-CGSTAB), are commonly used to obtain high-precision approximate solution. PCG is one of the most practical approximate methods based on the iterative solution process. Pre-conditioning is the most critical ingredient in PCG [16]. The original linear system is converted into a related system with a small condition number by introducing an appropriate pre-conditioning process. In this way, the total number of iterations required for solving the system to within some specified tolerances is reduced substantially. The

application of the PCG approach to reanalysis problems with an unchanged number of degrees of freedom (DOFs) has been proposed [17, 18]. Wu and Li [19] and Wu et al. [20] developed the PCG approach for static analysis of a structure with added DOFs where the nodes of the original structure form a subset of the nodes of the modified structure, using a particular effective pre-conditioner. Li and Wu [21] presented a PCG approach to structural static reanalysis for general layout modifications. The PCG method can perform structural reanalysis with high-rank modifications. Generally, the calculation amount of the Krylov subspace methods in each iteration step is related to the scale of the structural stiffness equation. In other words, the calculation amount of each iteration step will also be large when the total number of DOFs for an overall structure is large. Therefore, the combination of equation system reduction and the Krylov subspace methods is expected to achieve a more efficient static reanalysis. By combining system reduction with iterative solution, Li and Chen [22] proposed an efficient reanalysis method for structures with local modifications. In this approach, the reduced equation system of the modified structure is reconstructed according to the distribution of modified elements, and the pre-conditioned iterative solution algorithm is employed to solve the reduced equation system. Although excellent performance can be achieved in reanalysis for local modifications, Li and Chen's method is difficult to significantly improve the computational efficiency for the structures with high-rank modification, because the scale of the reduction system is still quite large. In order to realize the fast reanalysis for structures with high-rank modification, the system reduction method for the structures with global modification is required and further employed in the approximate reanalysis method.

In this paper, a system reduction-based approximate reanalysis method is developed for statically indeterminate structures with high-rank modification. In this method, a statically indeterminate structure is divided into the basis system (a statically determinate structure) and the additional components. Subsequently, the structural equilibrium equations are rewritten as the equation system with the stiffness matrix of the basis system and the pseudo forces introduced to express the influence of the additional elements. With the introduction of spectral decomposition, a reduced equation system with the element forces of the additional elements as the unknowns is

derived. Then, the approximate solutions of the modified structure can be obtained by solving the reduced equation system through a pre-conditioned iterative solution algorithm. The computational costs of the proposed method and the other two reanalysis methods are compared and numerical examples are presented to verify the effectiveness and efficiency of the proposed method.

2. Formulation

2.1. Decomposition of stiffness matrices

Regarding an element stiffness matrix, the spectral decomposition [8] is expressed as

$$\mathbf{K}_{(i)} = \mathbf{C}_{(i)}^T \mathbf{K}_{L(i)} \mathbf{C}_{(i)} \quad (1)$$

where $\mathbf{K}_{(i)}$ represents the stiffness matrix of the i -th element with the size of $n_{(i)} \times n_{(i)}$; $\mathbf{K}_{L(i)}$ indicates the $m_{(i)} \times m_{(i)}$ matrix composed of elemental stiffness parameters for the i -th element, with $m_{(i)}$ as the rank of $\mathbf{K}_{L(i)}$; $\mathbf{C}_{(i)}$ designates a transform matrix between the element stiffness matrix and the elemental stiffness parameters. The size of $\mathbf{C}_{(i)}$ is $m_{(i)} \times n_{(i)}$ and each line of $\mathbf{C}_{(i)}$ reflects the topological connectivity between DOFs for the corresponding elemental stiffness parameters in $\mathbf{K}_{L(i)}$. With respect to the structure with a given topology, $\mathbf{C}_{(i)}$ is considered to be invariant. Since the element stiffness matrix is not of full rank in most cases, $m_{(i)}$ is usually less than $n_{(i)}$. For the plane elements, $m_{(i)} = n_{(i)} - 3$ because there are two rigid body translation modes and one rigid body rotation mode; for the spatial elements, $m_{(i)} = n_{(i)} - 6$ because there are three rigid body translation modes and three rigid body rotation modes.

Regarding a structure composed of m elements, the stiffness matrix \mathbf{K} is expressed by the form of spectral decomposition as

$$\mathbf{K} = \sum_{i=1}^m \mathbf{K}_{(i)} = \sum_{i=1}^m \mathbf{C}_{(i)}^T \mathbf{K}_{L(i)} \mathbf{C}_{(i)} = \mathbf{C}^T \mathbf{K}_L \mathbf{C} \quad (2)$$

where the summation symbol $\sum_{i=1}^m(\cdot)$ denotes the conventional assembly of the m elements, \mathbf{K} represents an $n \times n$ matrix with n as the total number of DOFs of the structure, and \mathbf{K}_L refers to the matrix of structural stiffness parameters, which is a block diagonal matrix. The coefficients of \mathbf{K}_L are composed of the stiffness parameter matrices of all elements, namely,

$$\mathbf{K}_L = \sum_{i=1}^m \mathbf{K}_{L(i)} = \begin{bmatrix} \mathbf{K}_{L(1)} & \mathbf{0} & \cdots & \mathbf{0} \\ \mathbf{0} & \mathbf{K}_{L(2)} & \cdots & \mathbf{0} \\ \vdots & \vdots & \ddots & \vdots \\ \mathbf{0} & \mathbf{0} & \cdots & \mathbf{K}_{L(m)} \end{bmatrix} \quad (3)$$

In Eq. (2), \mathbf{C} represents the transform matrix between the matrix of structural stiffness parameters and the stiffness matrix of the whole structure, expressed as

$$\mathbf{C} = \sum_{i=1}^m \mathbf{C}_{(i)} = \begin{bmatrix} \tilde{\mathbf{C}}_{(1)}^T & \tilde{\mathbf{C}}_{(2)}^T & \cdots & \tilde{\mathbf{C}}_{(M)}^T \end{bmatrix}^T \quad (4)$$

Notably, $\tilde{\mathbf{C}}_{(i)} (i=1,2,\dots,m)$ denotes the extended matrix of $\mathbf{C}_{(i)} (i=1,2,\dots,m)$ for reflecting the topological connectivity between DOFs of the whole structure for the corresponding elemental stiffness parameters in $\mathbf{K}_{L(i)}$, and the size of $\tilde{\mathbf{C}}_{(i)} (i=1,2,\dots,m)$ is $m_{(i)} \times n$. $\tilde{\mathbf{C}}_{(i)} (i=1,2,\dots,m)$ is also invariant for the structure with given topology.

2.2. Reduced system of statically indeterminate structures

With respect to a structure with n DOFs, the equation system is expressed as

$$\mathbf{Kd} = \mathbf{R} \quad (5)$$

where \mathbf{R} and \mathbf{d} are the load vector and the structural displacement vector, respectively, and the size of both is $n \times 1$. The statically indeterminate structure is divided into two parts: the basis system and additional components. Generally, the basis system is a statically determinate structure, while the part of additional components consists of the components other than the basis system. Particularly, the additional components are distributed in the structure and are not required to form a

complete structural system. Corresponding to the basis system and the additional components, the stiffness matrix of the structure is classified into two parts. Then, Eq. (5) is further expressed as

$$(\mathbf{K}_b + \mathbf{K}_a)\mathbf{d} = \mathbf{R} \quad (6)$$

where \mathbf{K}_b and \mathbf{K}_a denote the stiffness matrices of the basis system and the additional components, respectively, and the size of both is $n \times n$. For the system without additional component, Eq. (6) can be expressed as $\mathbf{K}_b\mathbf{d} = \mathbf{R}$. Under the external loads, the additional components in the structure will produce deformations and internal forces. Using the similar concept given in the reference [23], the nodal forces generated by the additional components are regarded as the pseudo forces acting on the basis system. Then, Eq. (6) is further expressed as

$$\mathbf{K}_b\mathbf{d} = \mathbf{R} - \mathbf{K}_a\mathbf{d} \quad (7)$$

where $\mathbf{K}_a\mathbf{d}$ represents the pseudo nodal forces generated by the elements corresponding to the additional components. The expression of the displacement vector is obtained as

$$\mathbf{d} = \mathbf{K}_b^{-1}\mathbf{R} - \mathbf{K}_b^{-1}\mathbf{K}_a\mathbf{d} \quad (8)$$

With the expression in Eq. (2), \mathbf{K}_b and \mathbf{K}_a are expressed as

$$\mathbf{K}_b = \sum_{i \in \text{BASESYS}} \mathbf{K}_{(i)} = \sum_{i \in \text{BASESYS}} \mathbf{C}_{(i)}^T \mathbf{K}_{L(i)} \mathbf{C}_{(i)} = \mathbf{C}_b^T \mathbf{K}_{Lb} \mathbf{C}_b \quad (9)$$

$$\mathbf{K}_a = \sum_{i \in \text{ADDSYS}} \mathbf{K}_{(i)} = \sum_{i \in \text{ADDSYS}} \mathbf{C}_{(i)}^T \mathbf{K}_{L(i)} \mathbf{C}_{(i)} = \mathbf{C}_a^T \mathbf{K}_{La} \mathbf{C}_a \quad (10)$$

where BASESYS and ADDSYS represent the sets of elements in the basis system and the additional components, respectively; \mathbf{K}_{Lb} and \mathbf{K}_{La} indicate the matrices of stiffness parameters for the basis system and the additional components, respectively. In Eq. (9), \mathbf{C}_b and \mathbf{K}_{Lb} are both full rank matrices with the size of $n \times n$. Therefore, the inverse of \mathbf{K}_b is obtained by

$$\mathbf{K}_b^{-1} = \mathbf{C}_b^{-1} \mathbf{K}_{Lb}^{-1} \mathbf{C}_b^{-T} \quad (11)$$

By substituting Eqs. (11) and (10) into Eq. (8), the nodal displacement vector is expressed as

$$\mathbf{d} = \mathbf{C}_b^{-1} \mathbf{K}_{Lb}^{-1} \mathbf{C}_b^{-T} \mathbf{R} - \mathbf{C}_b^{-1} \mathbf{K}_{Lb}^{-1} \mathbf{C}_b^{-T} \mathbf{K}_a \mathbf{d} \quad (12)$$

In Eq. (12), $\mathbf{K}_a \mathbf{d}$ can be further expressed as

$$\mathbf{K}_a \mathbf{d} = \sum_{e \in \text{ADDSYS}} \mathbf{C}_{(e)}^T \mathbf{K}_{L(e)} \mathbf{u}_{(e)} = \mathbf{C}_a^T \mathbf{K}_{La} \mathbf{u}_a \quad (13)$$

where $\mathbf{u}_{(e)}$ represents the deformation displacement vector of the e -th element, corresponding to the stiffness parameters of the e -th element, and \mathbf{u}_a is expressed as

$$\mathbf{u}_a = \left[\mathbf{u}_{(1)}^T \quad \mathbf{u}_{(1)}^T \quad \cdots \quad \mathbf{u}_{(m)}^T \right]^T \quad (14)$$

where m refers to the number of elements corresponding to the additional components. By substituting Eq. (13) into Eq. (12), the nodal displacement vector is expressed by the deformation displacement vector of the additional components as

$$\mathbf{d} = \mathbf{C}_b^{-1} \mathbf{K}_{Lb}^{-1} \mathbf{C}_b^{-T} \mathbf{R} - \mathbf{C}_b^{-1} \mathbf{K}_{Lb}^{-1} \mathbf{C}_b^{-T} \mathbf{C}_a^T \mathbf{K}_{La} \mathbf{u}_a \quad (15)$$

Considering the relationship between the deformation displacement vector of an element and the structural nodal displacement vector:

$$\mathbf{u}_{(i)} = \tilde{\mathbf{C}}_{(i)} \mathbf{d}, \quad (16)$$

the expression of the deformation displacement vector of the additional components is obtained by substituting Eq. (15) into Eq. (16) and using the relationship in Eq. (14):

$$\mathbf{u}_a = \mathbf{C}_s \mathbf{K}_{Lb}^{-1} \mathbf{C}_b^{-T} \mathbf{R} - \mathbf{C}_s \mathbf{K}_{Lb}^{-1} \mathbf{C}_s^T \mathbf{K}_{La} \mathbf{u}_a \quad (17)$$

where

$$\mathbf{C}_s = \mathbf{C}_a \mathbf{C}_b^{-1} \quad (18)$$

By defining the deformation force vector corresponding to the deformation displacement vector of the additional components as

$$\mathbf{F}_a = \mathbf{K}_{La} \mathbf{u}_a \quad (19)$$

the deformation displacement vector \mathbf{u}_a can be expressed by \mathbf{F}_a as

$$\mathbf{u}_a = \mathbf{K}_{La}^{-1} \mathbf{F}_a \quad (20)$$

By substituting Eq. (20) into Eq. (17), the new equation system with the deformation force vector of the additional components as the unknowns is obtained as

$$\left(\mathbf{K}_{La}^{-1} + \mathbf{C}_s \mathbf{K}_{Lb}^{-1} \mathbf{C}_s^T\right) \mathbf{F}_a = \mathbf{C}_s \mathbf{K}_{Lb}^{-1} \mathbf{C}_b^{-T} \mathbf{R} \quad (21)$$

The size of the above equation system is $m_a = \sum_{e \in \text{ADDSYS}} m_{(e)}$, which is associated with the elements of the additional components. In the case of $m_a \leq n$, which applies to most engineering structures, the computational afford is significantly reduced by solving the new equation system (Eq.(21)) instead of the original equation system (Eq. (5)). Besides, only matrix \mathbf{K}_{La}^{-1} and matrix \mathbf{K}_{Lb}^{-1} in Eq. (21) need to be updated for any modified structure. \mathbf{K}_{La} and \mathbf{K}_{Lb} are both block diagonal matrices, and \mathbf{K}_{La}^{-1} and \mathbf{K}_{Lb}^{-1} are easily obtained by taking the inverse of each diagonal block of \mathbf{K}_{La} and \mathbf{K}_{Lb} . In other words, the coefficient matrix and the right-hand term of Eq. (21) are easily obtained without the time-consuming matrix inversion. It is worth mentioning that Eq. (21) can be easily solved by using a pre-conditioned iterative solution algorithm because the coefficient matrix of Eq. (21) is positive definite and symmetric.

To indicate the mechanical meaning of reduction system, Eq. (21) can be rewritten as $\mathbf{u}_a = \mathbf{K}_{La}^{-1} \mathbf{F}_a = \mathbf{C}_s \mathbf{K}_{Lb}^{-1} \mathbf{C}_b^{-T} \mathbf{R} - \mathbf{C}_s \mathbf{K}_{Lb}^{-1} \mathbf{C}_s^T \mathbf{F}_a$, which reflects the deformation compatibility condition on the additional components that the deformation of the additional components generated by the modified structure under the external loads is consistent with the deformation of the additional components generated by the basis system under the action of the external loads and the deformation force of the additional components.

2.3. Iterative solution for the reduced system

The Pre-conditioned Conjugate Gradient algorithm (PCG) is an iterative method for solving linear systems with positive definite and symmetric coefficient matrix. Practice has verified its high computational efficiency. By referring to the algorithm framework of PCG, this paper builds an iterative solution algorithm for the reduction system.

Generally, the right hand side of Eq. (21) is determined in advance and Eq. (21) is denoted as

$$\left(\mathbf{K}_{La}^{-1} + \mathbf{C}_s \mathbf{K}_{Lb}^{-1} \mathbf{C}_s^T\right) \mathbf{x} = \mathbf{B} \quad (22)$$

where $\mathbf{B} = \mathbf{C}_s \mathbf{K}_{Lb}^{-1} \mathbf{C}_b^T \mathbf{R}$ and $\mathbf{x} = \mathbf{F}_a$. Regarding the pre-conditioning, the pre-conditioner \mathbf{M} is set according to the state of the original structure, namely,

$$\mathbf{M} = \mathbf{C}_s \mathbf{K}_{Lb,0}^{-1} \mathbf{C}_s^T + \mathbf{K}_{La,0}^{-1}, \quad (23)$$

where $\mathbf{K}_{Lb,0}$ and $\mathbf{K}_{La,0}$ represent the original matrices of stiffness parameters of the basis system and the additional components, respectively. During the implementation of pre-conditioned iterative solution algorithm, \mathbf{M}^{-1} is obtained in advance and applied to the subsequent iterative solution.

The main steps of iterative solution for solving Eq. (22) are implemented as follows.

Step 1: Set an initial solution as $\mathbf{x}_0 = \mathbf{0}$ and set $j = 0$

Step 2: Compute the residual vector for the initial solution and the pre-conditioned residual vector

$$\mathbf{r}_0 = \mathbf{B} - \mathbf{K}_{La}^{-1} \mathbf{x}_0 - \mathbf{C}_s \mathbf{K}_{Lb}^{-1} \mathbf{C}_s^T \mathbf{x}_0, \quad \mathbf{z}_0 = \mathbf{M}^{-1} \mathbf{r}_0 \quad (24)$$

and the vector of search direction \mathbf{p}_0 can be obtained as $\mathbf{p}_0 = \mathbf{z}_0$.

Step 3: Update the solution through

$$\mathbf{x}_{j+1} = \mathbf{x}_j + \alpha_j \mathbf{p}_j \quad \text{where} \quad \alpha_j = (\mathbf{r}_j, \mathbf{z}_j) / (\mathbf{K}_{La}^{-1} \mathbf{p}_j + \mathbf{C}_s \mathbf{K}_{Lb}^{-1} \mathbf{C}_s^T \mathbf{p}_j, \mathbf{p}_j) \quad (25)$$

The operator $(\mathbf{v}_a, \mathbf{v}_b)$ represents the vector inner product of \mathbf{v}_a and \mathbf{v}_b .

Step 4: Update the residual vector \mathbf{r}_{j+1} and \mathbf{z}_{j+1} through

$$\mathbf{r}_{j+1} = \mathbf{r}_j - \alpha_j (\mathbf{K}_{La}^{-1} \mathbf{p}_j + \mathbf{C}_s \mathbf{K}_{Lb}^{-1} \mathbf{C}_s^T \mathbf{p}_j), \quad \mathbf{z}_{j+1} = \mathbf{M}^{-1} \mathbf{r}_{j+1} \quad (26)$$

Step 5: Update the vector of search direction \mathbf{p}_{j+1} through

$$\mathbf{p}_{j+1} = \mathbf{z}_{j+1} + \beta_j \mathbf{p}_j \quad \text{where} \quad \beta_j = (\mathbf{r}_{j+1}, \mathbf{z}_{j+1}) / (\mathbf{r}_j, \mathbf{z}_j) \quad (27)$$

Step 6: Check the condition of convergence. If $\|\mathbf{r}_j\| / \|\mathbf{B}\| < \varepsilon$, where ε represents the tolerance, the solution of the reduced system can be obtained as $\mathbf{F}_a = \mathbf{x}_{j+1}$. If $\|\mathbf{r}_j\| / \|\mathbf{B}\| \geq \varepsilon$, set $j = j + 1$ and transfer to **Step 3**. Once \mathbf{F}_a is obtained from the above algorithm, the displacement solution of the structure is obtained by

$$\mathbf{d} = \mathbf{C}_b^{-1} (\mathbf{K}_{Lb}^{-1} \mathbf{C}_b^T \mathbf{R} - \mathbf{K}_{Lb}^{-1} \mathbf{C}_s^T \mathbf{F}_a), \quad (28)$$

according to Eq. (20) and Eq. (15).

3. Computational cost

In this section, the computational cost of the proposed reanalysis method is studied, and compared with the other two existing reanalysis methods, which are also suitable for high-rank modification. For the sake of convenience, the three reanalysis methods considered are denoted as: (1) SRI, the proposed structural reanalysis method, which is based on System Reduction and Iterative solution; (2) PCG, the existing structural reanalysis method based on the Pre-conditioning Conjugate Gradient method [18, 19], (3) FDP, the structural reanalysis method based on Flexibility Disassembly Perturbation [8]. Considering that modern computing devices can usually provide enough storage space, this paper no longer considers the space complexity of computing methods. Then, the computational cost is quantified by the number of floating point operations (flops).

In the following analysis, the number of DOFs for the statically indeterminate structure is denoted as n . The scale of the matrix of stiffness parameters \mathbf{K}_{La} for the additional components is denoted as q . In order to simplify the analysis, this section only considers the case that the stiffness parameters for each element are uncoupled, so \mathbf{K}_{La} and \mathbf{K}_{Lb} are both diagonal matrices. For the case of coupled stiffness parameters, \mathbf{K}_{La} and \mathbf{K}_{Lb} may be block diagonal matrices and the computational cost will increase slightly, while the impact is small compared with the overall computational cost. The number of iterations required to reach the convergence condition is denoted as k for the reanalysis methods with iterative solution.

3.1. Flops of SRI

The implementation of reanalysis by using SRI can be divided into three stages: (A) Get initial vector; (B) Iterative solution for the reduced system; (C) Calculate the nodal displacement vector of the modified structure. Some matrices and vectors used in SRI, such as \mathbf{C}_s , \mathbf{C}_b , \mathbf{R} and \mathbf{M}^{-1} , can be determined in advance before the reanalysis operation. For the task of multiple reanalysis, these matrices remain unchanged and the computational cost of obtaining these matrices is relatively

small compared with the computational cost of multiple reanalysis. Therefore, the calculation amount of obtaining these matrices is not included in the computational cost. **Table 1** shows the number of flops for each formula used in SRI.

Table 1 Number of flops for the formulas in SRI.

Stage	Index	Formula	Number of flops
A	A-1	$\mathbf{B} = \mathbf{C}_s \mathbf{K}_{\text{Lb}}^{-1} \mathbf{C}_b^{-\text{T}} \mathbf{R}$	$2n^2 + 2nq + n$
	A-2	$\mathbf{r}_0 = \mathbf{B} - (\mathbf{K}_{\text{La}}^{-1} \mathbf{x}_0 + \mathbf{C}_s \mathbf{K}_{\text{Lb}}^{-1} \mathbf{C}_s^{\text{T}} \mathbf{x}_0)$	$2q^2 + 4nq + 2q + n$
	A-3	$\mathbf{z}_0 = \mathbf{M}^{-1} \mathbf{r}_0$	$2nq$
B	B-1	$\alpha_j = (\mathbf{r}_j, \mathbf{z}_j) / (\mathbf{K}_{\text{La}}^{-1} \mathbf{p}_j + \mathbf{C}_s \mathbf{K}_{\text{Lb}}^{-1} \mathbf{C}_s^{\text{T}} \mathbf{p}_j, \mathbf{p}_j)$	$2q^2 + 4nq + 5q + n + 1$
	B-2	$\mathbf{x}_{j+1} = \mathbf{x}_j + \alpha_j \mathbf{p}_j$	$2q$
	B-3	$\mathbf{r}_{j+1} = \mathbf{r}_j - \alpha_j (\mathbf{K}_{\text{La}}^{-1} \mathbf{p}_j + \mathbf{C}_s \mathbf{K}_{\text{Lb}}^{-1} \mathbf{C}_s^{\text{T}} \mathbf{p}_j)$	$2q^2 + 4nq + 3q + n$
	B-4	$\mathbf{z}_{j+1} = \mathbf{M}^{-1} \mathbf{r}_{j+1}$	$2q^2$
	B-5	$\beta_j = (\mathbf{r}_{j+1}, \mathbf{z}_{j+1}) / (\mathbf{r}_j, \mathbf{z}_j)$	$4q + 1$
	B-6	$\mathbf{p}_{j+1} = \mathbf{z}_{j+1} + \beta_j \mathbf{p}_j$	$2q$
C	C-1	$\mathbf{d} = \mathbf{C}_b^{-1} (\mathbf{K}_{\text{Lb}}^{-1} \mathbf{C}_b^{-\text{T}} \mathbf{R} - \mathbf{K}_{\text{Lb}}^{-1} \mathbf{C}_s^{\text{T}} \mathbf{F}_a)$	$2q^2 + 2nq + 2n$

It should be noted that most operations in SRI are carried out through multiplications of a matrix to a vector to reduce the number of flops, and no matrix multiplication is needed in the solution. For example, the specific calculation order and number of flops for formula (A-1) are

$$\mathbf{B} = \mathbf{C}_s \underbrace{\mathbf{K}_{\text{Lb}}^{-1} \mathbf{C}_b^{-\text{T}} \mathbf{R}}_{2n^2} \quad (29)$$

$$\underbrace{\quad}_{2n^2+n}$$

$$\underbrace{\quad}_{2n^2+n+2nq}$$

where the result of $\mathbf{K}_{\text{Lb}}^{-1} \mathbf{C}_b^{-\text{T}} \mathbf{R}$ can be denoted as \mathbf{B}_s and saved for the implementation of formula (C-1) in **Table 1**. Then, the specific calculation order and number of flops for formula (C-1) are

$$\mathbf{d} = \mathbf{C}_b^{-1} \left(\underbrace{\mathbf{B}_s - \mathbf{K}_{\text{Lb}}^{-1} \mathbf{C}_s^{\text{T}} \mathbf{F}_a}_{2nq+2n} \right) \quad (30)$$

$$\underbrace{\quad}_{2n^2+2nq+2n}$$

In addition, the calculation order and number of flops for $\mathbf{K}_{\text{La}}^{-1} \mathbf{x}_0 + \mathbf{C}_s \mathbf{K}_{\text{Lb}}^{-1} \mathbf{C}_s^{\text{T}} \mathbf{x}_0$ in formula (A-2) are

$$\underbrace{\underbrace{\mathbf{K}_{La}^{-1} \mathbf{x}_0}_{2q^2} + \mathbf{C}_s \underbrace{\mathbf{K}_{Lb}^{-1} \underbrace{\mathbf{C}_s^T \mathbf{x}_0}_{2nq}}_{2nq+n}}_{4nq+n} \quad (31)$$

$$\underbrace{\hspace{10em}}_{2q^2+4nq+n}$$

Similarly, the number of flops of $\mathbf{K}_{La}^{-1} \mathbf{p}_j + \mathbf{C}_s \mathbf{K}_{Lb}^{-1} \mathbf{C}_s^T \mathbf{p}_j$ in formulas (B-1) and (B-3) is $2q^2 + 4nq + n$.

The number of flops for vector inner product, such as $(\mathbf{r}_j, \mathbf{z}_j)$ in formulas (B-1) and (B-5), is $2q$.

According to the statistics of the number of flops in **Table 1**, the total number of flops for SRI with k iterations is

$$T_{F-SRI} = k(6q^2 + 8nq + 2n + 16q + 2) + 2n^2 + 4q^2 + 10nq + 4n + 2q \quad (32)$$

3.2. Flops of PCG and FDP

Compared with the proposed SRI, PCG [18, 19] directly solve Eq. (5) iteratively, where the scale of the equation system is n . In PCG, the original structural stiffness matrix is regarded as the pre-conditioner ($\mathbf{M} = \mathbf{K}_0$), and the inverse of the original structural stiffness matrix can be obtained and saved in advance. Similar to SRI, the calculation amount of obtaining \mathbf{M}^{-1} is not included in computational cost. The iteration process of PCG is similar to those of SRI, where the matrix $\mathbf{K}_{La}^{-1} + \mathbf{C}_s \mathbf{K}_{Lb}^{-1} \mathbf{C}_s^T$ is replaced by \mathbf{K} . The implementation of reanalysis by using PCG can be divided into two stages: (A) Get initial vector; (B) Iterative solution. The statistics similar to SRI are made and the total number of flops for PCG with k iterations is

$$T_{F-PCG} = k(6n^2 + 14n + 2) + 4n^2 + n \quad (33)$$

FDP [8] is another reanalysis method for structures with high-rank modification. This method reduces the calculation amount by distinguishing the basic system and additional components and using the spectral decomposition. This section analyzes the computational cost of FDP according to the expression in FDP, and points out the difference between FDP and SRI.

Firstly, the stiffness matrix of the modified structure is divided into

$$\mathbf{K} = \mathbf{K}_b + \mathbf{K}_a = \mathbf{K}_b + \mathbf{C}_a^T \mathbf{K}_{La} \mathbf{C}_a \quad (34)$$

Then, according to the SMW formulas used in FDP, the inverse of the stiffness matrix is

$$\mathbf{K}^{-1} = \mathbf{K}_b^{-1} - \mathbf{K}_b^{-1} \mathbf{C}_a^T \mathbf{K}_{La} \left(\mathbf{I} + \mathbf{C}_a \mathbf{K}_b^{-1} \mathbf{C}_a^T \mathbf{K}_{La} \right)^{-1} \mathbf{C}_a \mathbf{K}_b^{-1} \quad (35)$$

By substituting Eqs. (11) and (18) into Eq. (35), the expression of nodal displacement vector of the modified structure can be obtained by using Eq. (5) and expressed as

$$\mathbf{d} = \mathbf{K}^{-1} \mathbf{R} = \mathbf{C}_b^{-1} \left[\mathbf{K}_{Lb}^{-1} \mathbf{C}_b^{-T} \mathbf{R} - \mathbf{K}_{Lb}^{-1} \mathbf{C}_s^T \mathbf{K}_{La} \left(\mathbf{I} + \mathbf{C}_s \mathbf{K}_{Lb}^{-1} \mathbf{C}_s^T \mathbf{K}_{La} \right)^{-1} \mathbf{C}_s \mathbf{K}_{Lb}^{-1} \mathbf{C}_b^{-T} \mathbf{R} \right] \quad (36)$$

Comparing Eq. (36) with Eq. (28), the following equation should be true

$$\mathbf{F}_a = \mathbf{K}_{La} \left(\mathbf{I} + \mathbf{C}_s \mathbf{K}_{Lb}^{-1} \mathbf{C}_s^T \mathbf{K}_{La} \right)^{-1} \mathbf{C}_s \mathbf{K}_{Lb}^{-1} \mathbf{C}_b^{-T} \mathbf{R} \quad (37)$$

where \mathbf{I} is the identity matrix. In fact, the above equation is indeed true according to Eq. (19) and the following equation obtained by rewriting Eq. (17).

$$\left(\mathbf{C}_s \mathbf{K}_{Lb}^{-1} \mathbf{C}_s^T \mathbf{K}_{La} + \mathbf{I} \right) \mathbf{u}_a = \mathbf{C}_s \mathbf{K}_{Lb}^{-1} \mathbf{C}_b^{-T} \mathbf{R} \quad (38)$$

The difference between SRI and FDP should be noted. The former realizes system reduction by rewriting the equilibrium equations based on the concept of pseudo forces, while the latter obtains the expression of the inverse of stiffness matrix by directly using the given mathematical formulas (SMW formulas). The establishment of Eq. (37) verifies that the system reduction based on the concept of pseudo forces is correct. In other words, the derivation process of SRI clearly reflects the concepts of structural mechanics, and the derived reduction system also has clear physical significance. Meanwhile, the derivation process of this paper gives a mechanical explanation for the application of SMW formulas in structural reanalysis.

In order to count the number of flops in FDP, Eq. (36) can be rewritten as

$$\mathbf{d} = \mathbf{C}_b^{-1} \mathbf{K}_{Lb}^{-1} \left(\mathbf{P}_R - \mathbf{C}_s^T \mathbf{K}_{La} \mathbf{S}_a \mathbf{C}_s \mathbf{K}_{Lb}^{-1} \mathbf{P}_R \right) \quad (39)$$

where $\mathbf{P}_R = \mathbf{C}_b^{-T} \mathbf{R}$ and \mathbf{S}_a are

$$\mathbf{S}_a = \left(\mathbf{I} + \mathbf{C}_s \mathbf{K}_{Lb}^{-1} \mathbf{C}_s^T \mathbf{K}_{La} \right)^{-1} \quad (40)$$

Similar to SRI, \mathbf{P}_R , \mathbf{C}_b^{-1} and \mathbf{C}_s can be obtained in advance and the calculation amount of obtaining them is not included in computational cost. In other words, the flops of FDP are mainly included in Eqs. (40) and (39). The numbers of flops for Eqs. (40) and (39) can be determined by

$$\mathbf{S}_a = \left(\mathbf{I} + \underbrace{\mathbf{C}_s \mathbf{K}_{Lb}^{-1} \mathbf{C}_s^T \mathbf{K}_{La}}_{2nq^2+2nq} \right)^{-1} \mathbf{P}_R - \underbrace{\mathbf{C}_s^T \mathbf{K}_{La} \mathbf{S}_a \mathbf{C}_s \mathbf{K}_{Lb}^{-1} \mathbf{P}_R}_{2nq+n}, \quad \mathbf{d} = \underbrace{\mathbf{C}_b^{-1} \mathbf{K}_{Lb}^{-1} \mathbf{P}_R}_{2q^2+4nq+2n+q} - \underbrace{\mathbf{C}_s^T \mathbf{K}_{La} \mathbf{S}_a \mathbf{C}_s \mathbf{K}_{Lb}^{-1} \mathbf{P}_R}_{2q^2+2nq+n+q} \quad (41)$$

where the number of flops for the inverse of a $q \times q$ matrix is q^3 according to its $O(q^3)$ complexity. Then, the total number of flops for FDP is

$$T_{F-FDP} = 2nq^2 + q^3 + 2n^2 + 2q^2 + 6nq + 3n + 2q \quad (42)$$

3.3. Comparison study

This section presents a comparison of computational cost for SRI, PCG and FDP by using Eqs. (32), (33) and (42). Under the set of $n = 10000$, ratios of the flops of SRI to the other two methods under different settings of q and k are shown in **Fig. 1**. **Fig. 1a)** shows the comparison of the flops between SRI and PCG in the range of $q/n \in [0.05, 0.90]$ under the setting of $k_s = 0.1, 0.3, 0.5, 0.7$, where $k_s = k/q$ and $k_s = k/n$ for SRI and PCG, respectively. The results indicate that, with the reduction of the ratio of the reduced system size to the total number of DOFs, the computational cost of SRI will be significantly less than that of PCG, which is due to the significant reduction of the equation system to be solved. **Fig. 1b)** shows the comparison of the flops between SRI and FDP in the range of $k/q \in [0.01, 0.80]$ under the setting of $q/n = 0.1, 0.3, 0.5, 0.7$. The results indicate that, with the reduction of the ratio of the iteration number to the scale of reduced system, the computational cost of SRI can be significantly less than that of FDP. In other words, if the

approximate solution can be obtained in a small number of iterations through an effective iterative solution algorithm, SRI has significant advantage in solution efficiency.

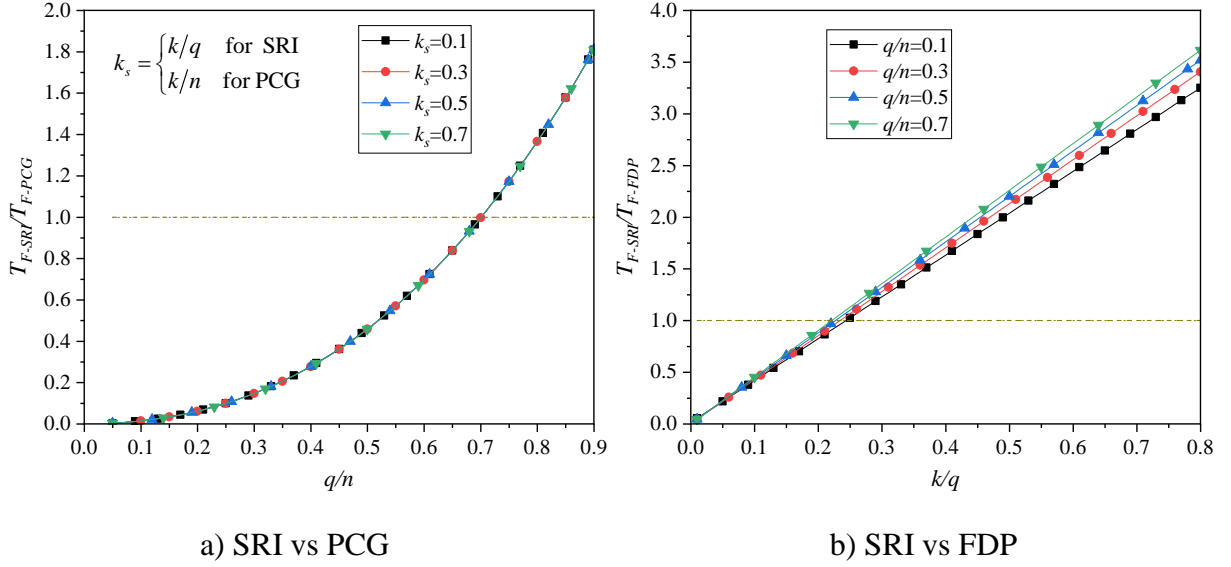


Fig. 1. Comparison of flops for different reanalysis methods.

4. Validation

Numerical examples are used to evaluate the computational performance of the proposed method. The solution algorithms have been programmed in MATLAB and run on a computer having an Intel® Core™ i7-8700 processor and a CPU at 3.2GHz with 64GB of RAM.

4.1. Truss structures with linear material

The two-dimensional truss structure with homogeneous material is adopted to evaluate the computational efficiency of the structural reanalysis methods. N_{span} and N_{floor} represent the total numbers of spans and floors, respectively. As suggested in **Fig. 2**, the span and the height of the floor are both set to 500cm. The value of the horizontal loads applying at the left nodes of the structure is set to $P = 20\text{kN}$. The cross-sectional area is set to 20 cm^2 for each truss element. In the original structure, Young's modulus is set to $E_0 = 20000\text{kN/cm}^2$ for all truss elements. Besides, Young's modulus is modified for structural reanalysis following the setting of the lower and upper values of Young's modulus (E_l and E_u). The value of Young's modulus is set gradually from the bottom floor to the top floor, with its lower and upper values of E_l and E_u , respectively. With a

structure of 5 floors as an example, the values of Young's modulus for the 1st-5th floors are 28000kN/cm², 25000kN/cm², 22000kN/cm², 19000kN/cm², and 16000kN/cm² under the setting of $E_1=16000\text{kN/cm}^2$ and $E_u=28000\text{kN/cm}^2$, respectively. For a structure with N_{span} spans, the diagonal bars in the 2nd - N_{span} th spans (Dotted lines) are defined as the additional components. Therefore, the number of additional components N_m and the ratio of N_m to the total number of DOFs are determined according to the setting of N_{span} . The tolerance for iterative solution algorithms is set to 1×10^{-12} .

A parameter a is used to determine the number of spans, floors, and the ratio of the number of additional components to the total number of DOFs, denoted by N_m/N_{DOF} . The relationships between N_{span} , N_{floor} , and a are expressed as

$$2^a - 1 = N_{\text{span}}, N_{\text{floor}} \times (N_{\text{span}} + 1) = N_{\text{node}} \quad (43)$$

where N_{node} represents the total number of unconstrained nodes of the structure. Considering different scales of numerical models with three total numbers of nodes ($N_{\text{node}} = 2048, 4096$ and 6144), the corresponding values are presented in **Table 2**.

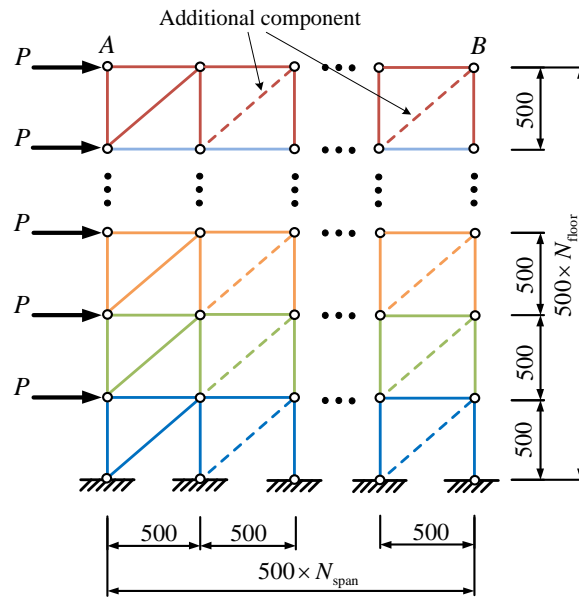


Fig. 2. The two-dimensional truss with N_{span} spans and N_{floor} floors (unit: cm).

Under the setting of $E_1 = 5000 \text{ kN/cm}^2$ and $E_u = 35000 \text{ kN/cm}^2$, the displacement solutions of the structure are obtained by FDP, PCG, SRI and the conventional method (regular complete analysis). With three scales of numerical models ($N_{\text{node}} = 2048, 4096$ and 6144), the displacements of nodes A and B under the setting of $N_{\text{span}} = 31$ are provided in **Table 3**. The results demonstrate that the displacement solutions obtained by the four methods are consistent, verifying the solution efficiency of the proposed method.

Table 2 Setting of number of spans and floors according to parameter a .

a	N_{span}	N_{floor}			N_m/N_{DOF}
		$N_{\text{node}} = 2048$	$N_{\text{node}} = 4096$	$N_{\text{node}} = 6144$	
1	1	1024	2048	3072	0.000
2	3	512	1024	1536	0.250
3	7	256	512	768	0.375
4	15	128	256	384	0.438
5	31	64	128	192	0.469
6	63	32	64	96	0.484

Table 3 Displacements of the truss with $N_{\text{span}} = 31$, $E_1 = 5000 \text{ kN/cm}^2$ and $E_u = 35000 \text{ kN/cm}^2$.

N_{node}	Method	Displacements of node A/cm		Displacements of node B/cm	
		Horizontal	Vertical	Horizontal	Vertical
2048	FDP	2.327843×10^1	3.694581×10^0	2.117298×10^1	-6.198756×10^0
	PCG	2.327843×10^1	3.694581×10^0	2.117298×10^1	-6.198756×10^0
	SRI	2.327843×10^1	3.694581×10^0	2.117298×10^1	-6.198756×10^0
	Conventional	2.327843×10^1	3.694581×10^0	2.117298×10^1	-6.198756×10^0
4096	FDP	2.485152×10^2	3.272211×10^1	2.462131×10^2	-4.393270×10^1
	PCG	2.485152×10^2	3.272211×10^1	2.462131×10^2	-4.393270×10^1
	SRI	2.485152×10^2	3.272211×10^1	2.462131×10^2	-4.393270×10^1
	Conventional	2.485152×10^2	3.272211×10^1	2.462131×10^2	-4.393270×10^1
6144	FDP	1.167079×10^3	1.161943×10^2	1.164704×10^3	-1.418954×10^2
	PCG	1.167079×10^3	1.161943×10^2	1.164704×10^3	-1.418954×10^2
	SRI	1.167079×10^3	1.161943×10^2	1.164704×10^3	-1.418954×10^2
	Conventional	1.167079×10^3	1.161943×10^2	1.164704×10^3	-1.418954×10^2

The Relative Computational Time (RCT) is defined as follows to evaluate the computational efficiency of the reanalysis methods.

$$\text{RCT} = T_{\text{reanalysis}} / T_c \quad (44)$$

where $T_{\text{reanalysis}}$ and T_c represent the computational times of the structural reanalysis method and the conventional method, respectively. The lower and upper values of Young's modulus are set to

$E_1 = 5000 \text{ kN/cm}^2$ and $E_u = 35000 \text{ kN/cm}^2$, reaching as much as 80% of the modification range of Young's modulus. In the cases of $N_{\text{node}} = 2048$, $N_{\text{node}} = 4096$ and $N_{\text{node}} = 6144$, the total number of structural DOFs are 4096, 8192, and 12288, respectively; the average computational times of the conventional method are 1.3374s, 9.5132s and 27.9936s, respectively. For the cases of $N_{\text{node}} = 2048$ and $N_{\text{node}} = 6144$, The relatively computational times of FDP, PCG and SRI under different settings of parameter a are presented in **Fig. 3**. The computational efficiency of these four structural reanalysis methods is summarized as follows.

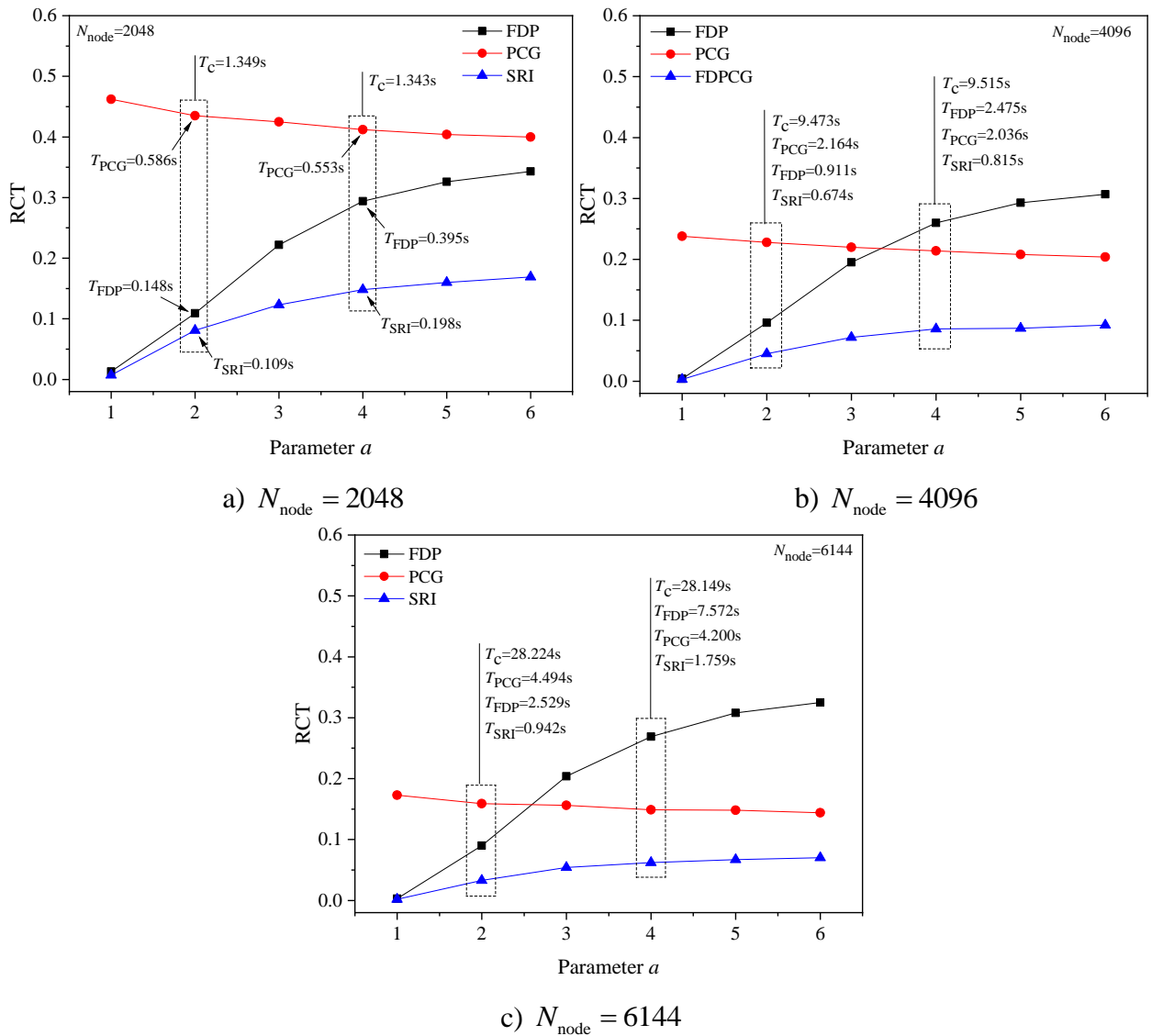


Fig. 3. RCT of the three reanalysis methods under different settings of parameter a .

FDP has high computational efficiency when N_m/N_{DOF} is relatively small, such as $N_m/N_{\text{DOF}} < 0.25$. With the increase in N_m/N_{DOF} , the RCT of FDP significantly increases, while

the solution efficiency remarkably decreases. This is that FDP still needs to solve large-scale linear equations by using the direction method (such as the Gauss elimination method) in these cases, leading to the increased computational time. For PCG, the computational efficiency is always higher than that of the conventional method and there is no significant relationship between the value of RCT and the value of N_m/N_{DOF} . The results in **Fig. 3** demonstrate that the computational efficiency of PCG is improved for large-scale structures. If the value of N_m/N_{DOF} is high and the scale of structural numerical models is large, the computational efficiency of PCG is higher than that of FDP.

Compared with FDP, SRI maintains high solution efficiency for the cases with a high value of N_m/N_{DOF} . The reason is that the pre-conditioned iterative solution method used in SRI can considerably reduce the computational time in solving the large-scale linear equations. Compared with PCG, SRI only needs to solve the linear system on a relatively small scale, with a less amount of calculation. In other words, SRI can give play to the advantages of system reduction and pre-conditioned iterative solution technology while maintaining high computational efficiency under different conditions. Besides, the RCT of SRI significantly decreases with the increase in the scale of the numerical model.

4.2. Frame structures with linear material

The two-dimensional frame structure (**Fig. 4**) is employed to demonstrate the effectiveness of the proposed method in the structural reanalysis of frame structures. As implied in **Fig. 4**, the span and the height of the floor are both set to 500cm. The value of the horizontal loads applying at the left nodes of the structure is set to $P = 20\text{kN}$. For each beam or column, the cross-section is set to $b \times h = 10\text{cm} \times 30\text{cm}$. The structure is simulated by using the beam finite element based on Euler-Bernoulli beam theory, and the number of beam elements used to model each beam is denoted by N_{sb} . **Fig. 4** provides the definition of the basis system and additional components for the frame structure with $N_{\text{sb}} = 2$, where the first beam element in each beam (the red element) is defined as the additional component.

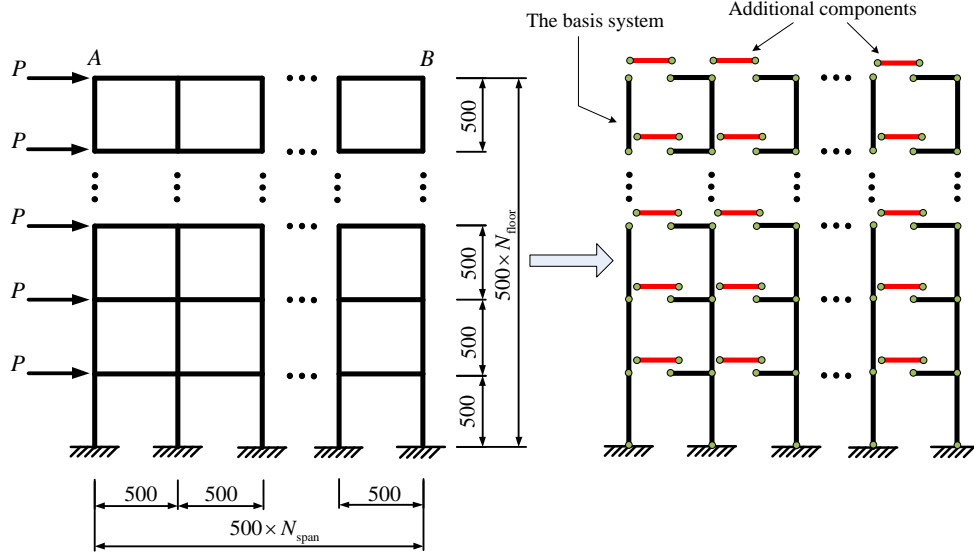


Fig. 4. The two-dimensional frame and its basis system and additional components (unit: cm).

(1) Homogeneous material

For the beams and columns with homogeneous material, the cross-sectional area and the moment of inertia of the cross-section are set to 300 cm^2 and 22500 cm^4 , respectively. For the original structure, Young's modulus is set to $E_0 = 20000\text{ kN/cm}^2$ for all elements. In the structural reanalysis, Young's modulus is modified according to the setting of the lower and upper values of Young's modulus (E_l and E_u). The value of Young's modulus is set gradually from the bottom floor to the top floor, with its lower and upper values of E_l and E_u , respectively, similar to the example in **Sec. 4.1**. Under different settings of N_{sb} , the total number of nodes N_{node} and the ratio of the number of additional components to the number of nodes, denoted by N_m/N_{node} , for the structure with $N_{span} = 50$, are listed in **Table 4**.

Regarding the implementation of reanalysis using FDP and SRI, the matrix of stiffness parameters for the e -th element $\mathbf{K}_{L(e)}$ is obtained as

$$\mathbf{K}_{L(e)} = \frac{1}{L_e^3} \begin{bmatrix} 2E_e A_e L_e^2 & 0 & 0 \\ 0 & 2E_e I_e L_e^2 & 0 \\ 0 & 0 & 6E_e I_e (L_e^2 + 4) \end{bmatrix} \quad (45)$$

where E_e , A_e , I_e , and L_e represent Young's modulus, cross-sectional area, the moment of inertia of the cross-section, and the length of the e -th element, respectively.

Table 4 Number of nodes and ratio of additional components under different of N_{sb} .

N_{sb}	N_{node}				N_m/N_{node}
	$N_{floor} = 20$	$N_{floor} = 30$	$N_{floor} = 40$	$N_{floor} = 50$	
1	1020	1530	2040	2550	0.980
2	2020	3030	4040	5050	0.495
3	3020	4530	6040	7550	0.331
4	4020	6030	8040	10050	0.249

Firstly, the solution accuracy of these reanalysis methods is examined by the structure with $N_{span} = 50$ and $N_{floor} = 20$, by taking the displacement solution of the conventional method (regular complete analysis) as a reference. Under $E_1 = 4000\text{kN/cm}^2$ and $E_u = 36000\text{kN/cm}^2$, the displacement solutions at node B under different values of N_{sb} are offered in **Table 5**, where the tolerance for PCG and SRI is set to 1×10^{-12} . The results indicate that the proposed method can obtain accurate displacement solutions since the four methods achieve consistent solutions.

Table 5 Displacements at node B of the frame structure with $N_{span} = 50$ and $N_{floor} = 20$.

N_{sb}	Methods	Horizontal displacement/cm	Vertical displacement/cm	Rotation/rad
1	FDP	3.444080×10^0	-3.476257×10^{-2}	-1.044827×10^{-4}
	PCG	3.444080×10^0	-3.476257×10^{-2}	-1.044827×10^{-4}
	SRI	3.444080×10^0	-3.476257×10^{-2}	-1.044827×10^{-4}
	Conventional	3.444080×10^0	-3.476257×10^{-2}	-1.044827×10^{-4}
2	FDP	3.444080×10^0	-3.476257×10^{-2}	-1.044827×10^{-4}
	PCG	3.444080×10^0	-3.476257×10^{-2}	-1.044827×10^{-4}
	SRI	3.444080×10^0	-3.476257×10^{-2}	-1.044827×10^{-4}
	Conventional	3.444080×10^0	-3.476257×10^{-2}	-1.044827×10^{-4}
3	FDP	3.444080×10^0	-3.476257×10^{-2}	-1.044827×10^{-4}
	PCG	3.444080×10^0	-3.476257×10^{-2}	-1.044827×10^{-4}
	SRI	3.444080×10^0	-3.476257×10^{-2}	-1.044827×10^{-4}
	Conventional	3.444080×10^0	-3.476257×10^{-2}	-1.044827×10^{-4}
4	FDP	3.444080×10^0	-3.476257×10^{-2}	-1.044827×10^{-4}
	PCG	3.444080×10^0	-3.476257×10^{-2}	-1.044827×10^{-4}
	SRI	3.444080×10^0	-3.476257×10^{-2}	-1.044827×10^{-4}
	Conventional	3.444080×10^0	-3.476257×10^{-2}	-1.044827×10^{-4}

Furthermore, the solution efficiency of FDP, PCG, and SRI is evaluated. With different settings of N_{sb} and N_{floor} , the computational times of the conventional method and the relative

computational times of FDP, PCG, and SRI are presented in **Table 6**. The results in **Table 6** are discussed as follows. In the cases of $N_{sb}=1$ and $N_{sb}=2$, the scale of the reduction system reconstructed based on additional components is relatively large, making the advantages of system reduction in FDP and SRI unable to be fully reflected. Therefore, PCG achieves the highest computational efficiency in these cases. The computational efficiency of FDP and SRI is significantly improved when the scale of the reduction system reconstructed based on additional components is relatively small, such as $N_{sb}=3$ and $N_{sb}=4$. The solution efficiency of FDP may be lower than that of PCG (such as the case of $N_{sb}=3$ and $N_{floor} > 20$) with the increase in the total number of DOFs. The reason is that a large amount of calculation is still required to solve the large-scale reduction system with the direct solution method.

Table 6 Comparison of solution efficiency between different methods ($N_{span} = 50$).

$N_{sb} (N_m/N_{node})$	N_{floor}	N_{DOF}	T_c/s	RCT		
				FDP	PCG	SRI
1 (0.980)	10	1530	0.059	2.515	0.785	2.601
	20	3060	0.373	2.335	0.641	1.744
	30	4590	1.306	2.198	0.441	1.089
	40	6120	2.879	2.175	0.365	0.863
	50	7650	5.470	2.156	0.303	0.705
2 (0.495)	10	3030	0.370	0.585	0.578	0.744
	20	6060	2.853	0.478	0.329	0.385
	30	9090	9.023	0.466	0.244	0.265
	40	12120	21.143	0.432	0.194	0.199
	50	15150	40.509	0.419	0.157	0.161
3 (0.331)	10	4530	1.168	0.238	0.405	0.339
	20	9060	9.166	0.192	0.228	0.170
	30	13590	29.985	0.181	0.165	0.114
	40	18120	69.152	0.175	0.131	0.085
	50	22650	139.444	0.167	0.103	0.068
4 (0.249)	10	6030	2.868	0.123	0.292	0.186
	20	12060	21.604	0.110	0.173	0.095
	30	18090	71.509	0.104	0.126	0.064
	40	24120	156.277	0.102	0.106	0.049
	50	30150	332.567	0.090	0.102	0.038

Different from FDP, SRI avoids the problem of reduced computational efficiency caused by the increase in the scale of the reduced system, by adopting the pre-conditioned iterative method to solve the reduced system. Therefore, SRI maintains high computational efficiency in the cases of large-scale numerical models. As suggested in **Table 6**, the advantage in computational efficiency

of SRI becomes more and more significant with the decrease in the proportion of additional components and the increase in the scale of the numerical model.

(2) Functionally graded material

The application of functionally graded (FG) structures in aerospace, marine, civil construction is growing rapidly due to their high strength-to-weight ratio [24]. In order to ensure the accuracy of numerical simulation, a refined mesh is usually required for modeling the FG structures by using finite element method, which will greatly increase the amount of calculation in finite element solution and bring great difficulties to structural optimization and reliability assessment that need repeated finite element solution. Fast reanalysis of the modified FG structures has become a meaningful work, which provides important support for efficient optimization design and reliability assessment of FG structures.

The effective Young's modulus of the FG beams is assumed to vary continuously through the beam depth by a power-law as [25, 26]:

$$E(y) = (E_{US} - E_{LS}) \left(\frac{y}{h} + \frac{1}{2} \right)^p + E_{LS}, \quad -\frac{h}{2} \leq y \leq \frac{h}{2} \quad (46)$$

where $E(y)$ represents the Young's modulus of the FG material at location y along with the height, E_{US} , E_{LS} denote the generic material properties at upper and lower surfaces of the FG beam, respectively; h refers to the height of the FG beam, p is the power-law exponent.

A variety of different beam models have been established to conduct analysis of FG beams, such as Euler-Bernoulli beam model [26, 27], first-order shear beam model [25, 28, 29] and higher-order shear beam model [24, 30-32]. In this study, the Euler Bernoulli beam model is selected and the stiffness matrix of the i -th FG beam element in local coordinate system is expressed as [26, 27]

$$\mathbf{K}_{c(i)} = \frac{1}{L_i^3} \begin{bmatrix} A_{Ei} b_i L_i^2 & 0 & -B_{Ei} b_i L_i^2 & -A_{Ei} b_i L_i^2 & 0 & B_{Ei} b_i L_i^2 \\ 0 & 12D_{Ei} b_i & 6D_{Ei} b_i L_i & 0 & -12D_{Ei} b_i & 6D_{Ei} b_i L_i \\ -B_{Ei} b_i L_i^2 & 6D_{Ei} b_i L_i & 4D_{Ei} b_i L_i^2 & B_{Ei} b_i L_i^2 & -6D_{Ei} b_i L_i & 2D_{Ei} b_i L_i^2 \\ -A_{Ei} b_i L_i^2 & 0 & B_{Ei} b_i L_i^2 & A_{Ei} b_i L_i^2 & 0 & -B_{Ei} b_i L_i^2 \\ 0 & -12D_{Ei} b_i & -6D_{Ei} b_i L_i & 0 & 12D_{Ei} b_i & -6D_{Ei} b_i L_i \\ B_{Ei} b_i L_i^2 & 6D_{Ei} b_i L_i & 2D_{Ei} b_i L_i^2 & -B_{Ei} b_i L_i^2 & -6D_{Ei} b_i L_i & 4D_{Ei} b_i L_i^2 \end{bmatrix} \quad (47)$$

where

$$A_{Ei} = \frac{h_i}{p_i + 1} E_{US}^i + \frac{h_i p_i}{p_i + 1} E_{LS}^i \quad (48)$$

$$B_{Ei} = \frac{h_i^2}{2(p_i + 1)(p_i + 2)} E_{US}^i - \frac{h_i^2}{2(p_i + 1)(p_i + 2)} E_{LS}^i \quad (49)$$

$$D_{Ei} = \frac{h_i^3 (p_i^2 + p_i + 2)}{4(p_i + 1)(p_i + 2)(p_i + 3)} E_{US}^i + \left[\frac{h_i^3}{12} - \frac{h_i^3 (p_i^2 + p_i + 2)}{4(p_i + 1)(p_i + 2)(p_i + 3)} \right] E_{LS}^i \quad (50)$$

With the transform matrix between the stiffness matrix and stiffness parameters in local coordinate system [8] used, the matrix of elemental stiffness parameters for the FG beam element can be obtained as

$$\mathbf{K}_{L(i)} = \mathbf{C}_{c(i)} \mathbf{K}_{c(i)} \mathbf{C}_{c(i)}^T = \begin{bmatrix} k_{11}^{(i)} & k_{12}^{(i)} & 0 \\ k_{12}^{(i)} & k_{22}^{(i)} & 0 \\ 0 & 0 & k_{33}^{(i)} \end{bmatrix} = \begin{bmatrix} 2A_{Ei} b_i / L_i & -2B_{Ei} b_i / L_i & 0 \\ -2B_{Ei} b_i / L_i & 2D_{Ei} b_i / L_i & 0 \\ 0 & 0 & 6(L_i^2 + 4) D_{Ei} b_i / L_i^3 \end{bmatrix} \quad (51)$$

It can be realized that $k_{12}^{(i)}$ reflects the coupling effect of axial deformation and flexural deformation. The comparison between Eq. (45) and Eq. (51) indicates that, different from the element with homogeneous material, $\mathbf{K}_{L(i)}$ of the FG beam element is no longer a diagonal matrix, due to the coupling of element stiffness parameters.

The two-dimensional frame structure (**Fig. 4**) is taken into consideration, and the columns and beams of the frame are assumed to be made of FG material, with the effective Young's modulus varied continuously through the height of the cross-section. Especially, E_{LS} and E_{US} represent the values of Young's modulus at upper and lower surfaces of the beams, respectively, or at right and left surfaces of the columns, respectively. For the original structure, E_{LS} and E_{US} are set to the same value as $E_{LS} = E_{US} = E_0 = 20000 \text{ kN/cm}^2$ and the power-law exponent is set as $p = 1.0$ for all elements. For the reanalysis, the structure is modified by changing the value of $E_{US} \in [E_l, E_u]$. The value of E_{US} is set gradually from the bottom floor to the top floor, with its lower and upper values of E_l and E_u , respectively. In numerical modeling, each column or beam is modelled by using 8

FG beam elements so as to obtain acceptable approximate displacement solutions, based on the investigation given by Li et al. (See Table 3 in Ref. [24]).

Taking the displacement solution of the conventional method (regular complete analysis) as a reference, the solution accuracy of these reanalysis methods is examined by using the frame structure with $N_{\text{span}} = N_{\text{floor}} = 4$. Under $E_1 = 4000 \text{ kN/cm}^2$ and $E_u = 36000 \text{ kN/cm}^2$, the displacement solutions at node B under different settings of power-law exponent are shown in **Table 7**, where the tolerance for PCG and SRI is set to 1×10^{-12} . It can be seen that the proposed method can obtain accurate displacement solutions, which indicates that the expressions of stiffness parameters for the functionally graded beam element, derived by the transformation matrix obtained from the spectral decomposition of the homogeneous material beam element, are reliable.

Table 7 Displacements at node B of the frame with $N_{\text{span}} = N_{\text{floor}} = 4$.

p	Methods	Horizontal displacement/cm	Vertical displacement/cm	Rotation/rad
0.5	FDP	2.111726×10^0	-5.859733×10^{-2}	-8.018189×10^{-4}
	PCG	2.111726×10^0	-5.859733×10^{-2}	-8.018189×10^{-4}
	SRI	2.111726×10^0	-5.859733×10^{-2}	-8.018189×10^{-4}
	Conventional	2.111726×10^0	-5.859733×10^{-2}	-8.018189×10^{-4}
1.0	FDP	1.757305×10^0	-7.509972×10^{-2}	-3.540270×10^{-4}
	PCG	1.757305×10^0	-7.509972×10^{-2}	-3.540270×10^{-4}
	SRI	1.757305×10^0	-7.509972×10^{-2}	-3.540270×10^{-4}
	Conventional	1.757305×10^0	-7.509972×10^{-2}	-3.540270×10^{-4}
2.0	FDP	1.717977×10^0	-6.925002×10^{-2}	-2.863039×10^{-4}
	PCG	1.717977×10^0	-6.925002×10^{-2}	-2.863039×10^{-4}
	SRI	1.717977×10^0	-6.925002×10^{-2}	-2.863039×10^{-4}
	Conventional	1.717977×10^0	-6.925002×10^{-2}	-2.863039×10^{-4}

The solution efficiency of FDP, PCG, SRI and the conventional method is investigated by the structures with $N_{\text{span}} = 10$. With different settings of N_{floor} and the power-law exponent p , the computational times of different methods are presented in **Table 8**. It is worth noting that the ratio of the number of additional components to the total number of DOFs is $N_m/N_{\text{DOF}} = 0.063$ for all cases in **Table 8**. In this case, FDP and SRI can significantly reduce the computational time, which is also proved by the results in the table. It can be seen from the data given by **Table 8** that SRI has the highest solution efficiency, which indicates that the proposed reanalysis method has good

performance for modification of statically indeterminate structures composed of functionally graded beams. Further statistics on the results in **Table 8** show that, the relative computational time of SRI defined by T_{SRI}/T_c is about 4.89%, 3.46%, 2.34% and 1.88%, respectively, for the four structural scales where the total number of structural DOFs is 4740, 9480, 14220 and 18960, respectively. It means that, with the increase of the structural scale, the solution efficiency of SRI is improved more and more significantly.

Table 8 Comparison of solution efficiency between different methods ($N_{\text{span}} = 10$).

p	N_{floor}	N_{DOF}	T_c/s	T_{FDP}/s	T_{PCG}/s	T_{SRI}/s
0.5	10	4740	1.420	0.157	0.761	0.069
	20	9480	11.034	0.931	3.510	0.379
	30	14220	35.562	2.826	8.204	0.842
	40	18960	83.397	6.665	14.856	1.649
1.0	10	4740	1.446	0.153	0.517	0.067
	20	9480	11.411	0.964	2.107	0.379
	30	14220	36.822	2.954	4.725	0.824
	40	18960	85.889	6.827	8.568	1.474
2.0	10	4740	1.415	0.143	0.388	0.075
	20	9480	11.115	0.937	1.575	0.395
	30	14220	35.717	2.913	3.617	0.842
	40	18960	83.944	6.706	6.479	1.613
5.0	10	4740	1.431	0.155	0.326	0.068
	20	9480	11.145	0.924	1.320	0.391
	30	14220	35.887	2.823	2.964	0.888
	40	18960	83.704	6.669	5.214	1.565
10.0	10	4740	1.571	0.157	0.283	0.077
	20	9480	11.334	0.971	1.177	0.394
	30	14220	37.463	2.816	2.561	0.857
	40	18960	83.732	6.385	4.477	1.588

4.3. Truss structures with nonlinear material

In this section, the two-dimensional truss structure with homogeneous material (**Fig. 2**) is assumed to be made of nonlinear material to evaluate the application effect of the proposed reanalysis method for structural static nonlinear analysis. The bilinear material model used in Ref. [22] is employed, where E_0 and E_t represent Young's modulus and the tangent modulus, respectively, and σ_y refers to the yield stress. Young's modulus and the tangent modulus are set to $E_0 = 2 \times 10^5 \text{ kN/cm}^2$ and $E_t = 0.3 \times 10^5 \text{ kN/cm}^2$, respectively. The cross-sectional area of all elements is set to 200 cm^2 .

For static nonlinear analysis, the equilibrium equations of the structure are expressed as

$$\mathbf{F}(\mathbf{d}) - \lambda \mathbf{P}_0 = \mathbf{0} \quad (52)$$

where \mathbf{P}_0 represents the constantly applied force vector, and λ indicates the load factor. The Newton-Raphson method with load control [33] is employed to solve the above nonlinear equation. In the implement of Newton-Raphson method, the following incremental equations are required to be repeatedly solved.

$$\mathbf{K}_t|_{\mathbf{d}=\mathbf{d}^*} \Delta \mathbf{d} = -\mathbf{R}_r(\mathbf{d}^*) \quad (53)$$

where $\mathbf{K}_t|_{\mathbf{d}=\mathbf{d}^*}$ indicates the tangent stiffness matrix of the structure and $\mathbf{R}_r(\mathbf{d}) = \mathbf{F}(\mathbf{d}) - \lambda \mathbf{P}_0$ is the residual force vector of the structure. In this work, the proposed reanalysis method is employed to solve the above-linearized equation.

Three methods are employed to obtain the incremental displacements for implementation of the incremental-iteration procedure: (1) NR-Regular, the incremental displacements are obtained by solving Eq. (53) with the Gauss elimination algorithm used; (2) NR-Reduction, the incremental displacements are obtained by solving Eq. (21) with Gauss elimination algorithm used; (3) NR-SRI, the incremental displacements are obtained by using the proposed reanalysis method. The convergence condition for iteration in the Newton-Raphson method is set to $\|\mathbf{R}_r\|/\|\lambda \mathbf{P}_0\| < 1 \times 10^{-8}$. For NR-SRI, the convergence condition for iteration is set to $\|\mathbf{r}_j\|/\|\lambda \mathbf{P}_0\| < 1 \times 10^{-15}$.

Let $N_{\text{span}} = 30$ and $N_{\text{floor}} = 150$, the numbers of DOFs and the finite element of the whole numerical model are 9300 and 13650, respectively. The basic value of the load is set to $P_0 = 500\text{kN}$ and 20 load steps with equal incremental load (25kN) are adopted to obtain the displacement solutions of the structure. In three yield stress cases of $\sigma_y = 45\text{kN/cm}^2$, $\sigma_y = 25\text{kN/cm}^2$, and $\sigma_y = 5\text{kN/cm}^2$, the relation curves between the horizontal displacement of node *B* and the load factor obtained by the Newton-Raphson method with the three ways to obtain the incremental displacements are illustrated in **Fig. 5**. It can be revealed that the displacement solutions obtained by NR-Regular, NR-Reduction, and NR-SRI are consistent. Thus, the proposed reanalysis method is well introduced into the solution algorithm for structural nonlinear analysis without reducing the solution accuracy of the algorithm.

Table 9 illustrates the computational time required by NR-Regular, NR-Reduction, and NR-SRI, as well as the total number of nonlinear elements under the three settings of yield stress. **Table 9** demonstrates that the nonlinear analysis algorithm with the proposed reanalysis method has the highest solution efficiency, the computational time of which is about 10% of that needed by NR-Regular and 28% of that needed by NR-Reduction. Compared with NR-Regular, the improvement of NR-Reduction in computational efficiency is derived from the reduction of the scale of linear equations to be solved in the nonlinear analysis process. Compared with NR-Reduction, the improvement of NR-SRI in computational efficiency reflects the high efficiency of using pre-conditioned conjugate gradient method to solve linear equations. In the cases with different numbers of nonlinear elements, NR-SRI stably presents high computational performance, verifying that the reanalysis method proposed in this paper can play a positive role in the static nonlinear analysis of structures.

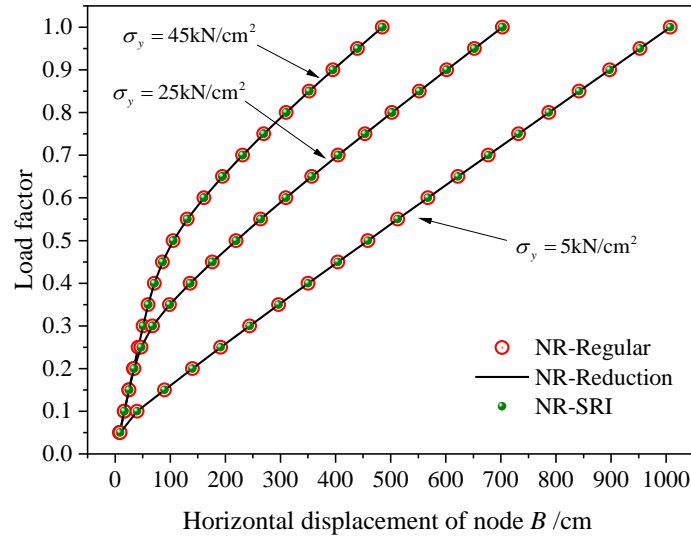


Fig. 5. Relation curves between displacement and load factor.

Table 9 Comparison of solution efficiency for NR-Regular, NR-Reduction and NR-SRI.

$\sigma_y / \text{kN/cm}^2$	N_{NLE}	$T_{\text{NR-Regular}} / \text{s}$	$T_{\text{NR-Reduction}} / \text{s}$	$T_{\text{NR-SRI}} / \text{s}$
45	1691	689.610	225.257	61.203
25	2567	794.655	265.741	72.963
5	9116	937.395	321.751	95.491

Note: N_{NLE} represents the total number of nonlinear elements, $T_{\text{NR-Regular}}$, $T_{\text{NR-Reduction}}$ and $T_{\text{NR-SRI}}$ are the total computational time for NR-Regular, NR-Reduction and NR-SRI, respectively.

5. Conclusions

In this paper, a system reduction-based approximate reanalysis method is developed for statically indeterminate structures with high-rank modification. The analysis of computational cost and numerical examples are presented. The conclusions are drawn as follows.

(1) Based on the division of basis system and additional components and the introduction of spectral decomposition, the reduced equation system of statically indeterminate structures can be successfully established, which provides support for implementation of fast approximate reanalysis method. Different from the flexibility disassembly perturbation method which is based on the given mathematical formulas (SMW formulas), the present derivation has clear mechanical significance, and gives a mechanical explanation for the application of SMW formulas in structural reanalysis.

(2) The proposed reanalysis method realizes the integration of system reduction and iterative solution. The numerical results indicate that the proposed method has high computational performance for statically indeterminate structures with high-rank modification, due to its advantages of system reduction and fast iterative solution. Generally, the advantage of solution efficiency of the proposed method becomes increasingly significant with the increase in the scale of the numerical model. The combination of system reduction and pre-conditioned iterative solution can be regarded as a promising model for developing high-performance reanalysis methods.

(3) For the statically indeterminate structures made of functionally graded material, where multiple beam elements are required to model each column and beam, the proposed system reduction method can significantly reduce the equation system to be solved and hence the proposed reanalysis method achieve excellent computational performance. The results of numerical examples indicate that the proposed method still has high computational performance in the case of coupled element stiffness parameters.

(4) The proposed reanalysis method can be applied to improve the performance of static nonlinear analysis for statically indeterminate structures with nonlinear materials.

Acknowledgments

The project is funded by the National Natural Science Foundation of China (Grant No. 52178209) and Guangdong Basic and Applied Basic Research Foundation, China (Grant No. 2020A1515010611, Grant No. 2021A1515012280).

References

- [1] Koohestani K. Structural reanalysis via force method. *International Journal of Solids and Structures* 2018; 136-137: 103-11.
- [2] Akgün MA, Garcelon JH, Haftka RT. Fast exact linear and non-linear structural reanalysis and the Sherman–Morrison–Woodbury formulas. *International Journal for Numerical Methods in Engineering* 2001; 50: 1587-606.
- [3] Hager WW. Updating the inverse of a matrix. *Siam Review* 1989; 31: 221-39.
- [4] Sack RL, Carpenter WC, Hatch GL. Modification of elements in the displacement method. *AIAA Journal* 1967; 5: 1708-10.
- [5] Kirsch U, Rubinstein MF. Reanalysis for limited structural design modifications. *Journal of the Engineering Mechanics Division* 1972; 98: 61-70.
- [6] Huang C, Verchery G. An exact structural static reanalysis method. *Communications in Numerical Methods in Engineering* 1997; 13: 103-12.
- [7] Deng L, Ghosn M. Pseudoforce method for nonlinear analysis and reanalysis of structural systems. *Journal of Structural Engineering -ASCE* 2001; 127: 570-78.
- [8] Yang QW. Fast and exact algorithm for structural static reanalysis based on flexibility disassembly perturbation. *AIAA Journal* 2019; 57: 3599-607.
- [9] Song Q, Chen P, Sun S. An exact reanalysis algorithm for local non-topological high-rank structural modifications in finite element analysis. *Computers & Structures* 2014; 143: 60-72.
- [10] Gao G, Wang H, Li E, Li G. An exact block-based reanalysis method for local modifications. *Computers & Structures* 2015; 158: 369-80.
- [11] Jensen HA, Muñoz A, Papadimitriou C, Vergara C. An enhanced substructure coupling technique for dynamic re-analyses: Application to simulation-based problems. *Computer Methods in Applied Mechanics and Engineering* 2016; 307: 215-34.
- [12] Kirsch U. Combined approximations – a general reanalysis approach for structural

- optimization. *Structural and Multidisciplinary Optimization* 2000; 20: 97-106.
- [13] Kirsch U. *Reanalysis of Structures--A Unified Approach for Linear, Nonlinear, Static and Dynamic Systems*. Springer, 2008.
- [14] Kirsch U. Reanalysis and sensitivity reanalysis by combined approximations. *Structural and Multidisciplinary Optimization* 2010; 40: 1-15.
- [15] Saad Y. *Iterative Methods for Sparse Linear Systems*. 2 ed. Boston: PWS Pub. Co, 2003.
- [16] Benzi M. Preconditioning techniques for large linear systems: A Survey. *Journal of Computational Physics* 2002; 182: 418-77.
- [17] Noor AK, Whitworth SL. Reanalysis procedure for large structural systems. *International Journal for Numerical Methods in Engineering* 1988; 26: 1729-48.
- [18] Kirsch U, Kocvara M, Zowe J. Accurate reanalysis of structures by a preconditioned conjugate gradient method. *International Journal for Numerical Methods in Engineering* 2002; 55: 233-51.
- [19] Wu BS, Li ZG. Static reanalysis of structures with added degrees of freedom. *Communications in Numerical Methods in Engineering* 2006; 22: 269-81.
- [20] Wu B, Lim CW, Li Z. A finite element algorithm for reanalysis of structures with added degrees of freedom. *Finite Elements in Analysis and Design* 2004; 40: 1791-801.
- [21] Li Z, Wu B. A preconditioned conjugate gradient approach to structural reanalysis for general layout modifications. *International Journal for Numerical Methods in Engineering* 2007; 70: 505-22.
- [22] Li W, Chen S. Structural reanalysis method for local modifications based on system reduction and iterative solution. *Engineering Structures* 2022; 273: 114977.
- [23] Li W, Ma H. A novel model order reduction scheme for fast and accurate material nonlinear analyses of large-scale engineering structures. *Engineering Structures* 2019; 193: 238-57.
- [24] Li W, Ma H, Gao W. A higher-order shear deformable mixed beam element model for accurate analysis of functionally graded sandwich beams. *Composite Structures* 2019; 221: 110830.
- [25] Nguyen T, Vo TP, Thai H. Static and free vibration of axially loaded functionally graded beams based on the first-order shear deformation theory. *Composites Part B: Engineering* 2013; 55: 147-57.
- [26] Wu D, Gao W, Gao K, Tin-Loi F. Robust safety assessment of functionally graded structures with interval uncertainties. *Composite Structures* 2017; 180: 664-85.
- [27] Lee JW, Lee JY. Free vibration analysis of functionally graded Bernoulli-Euler beams using an exact transfer matrix expression. *International Journal of Mechanical Sciences* 2017; 122:

1-17.

- [28] Li S, Batra RC. Relations between buckling loads of functionally graded Timoshenko and homogeneous Euler–Bernoulli beams. *Composite Structures* 2013; 95: 5-09.
- [29] Li W, Ma H, Gao W. Geometrically exact beam element with rational shear stress distribution for nonlinear analysis of FG curved beams. *Thin-Walled Structures* 2021; 164: 107823.
- [30] Filippi M, Carrera E, Zenkour AM. Static analyses of FGM beams by various theories and finite elements. *Composites Part B: Engineering* 2015; 72: 1-09.
- [31] Thai H, Vo TP. Bending and free vibration of functionally graded beams using various higher-order shear deformation beam theories. *International Journal of Mechanical Sciences* 2012; 62: 57-66.
- [32] Li W, Gao W, Chen S. A material-based higher-order shear beam model for accurate analyses of FG beams with arbitrary material distribution. *Composite Structures* 2020; 245: 112253.
- [33] Crisfield MA. *Non-linear Finite Element Analysis of Solids and Structures vol. 1: Essentials*. Chichester: John Wiley & Sons, 1991.